Supplementary Figure S1. Nuclear CPD fluorescence quantification.

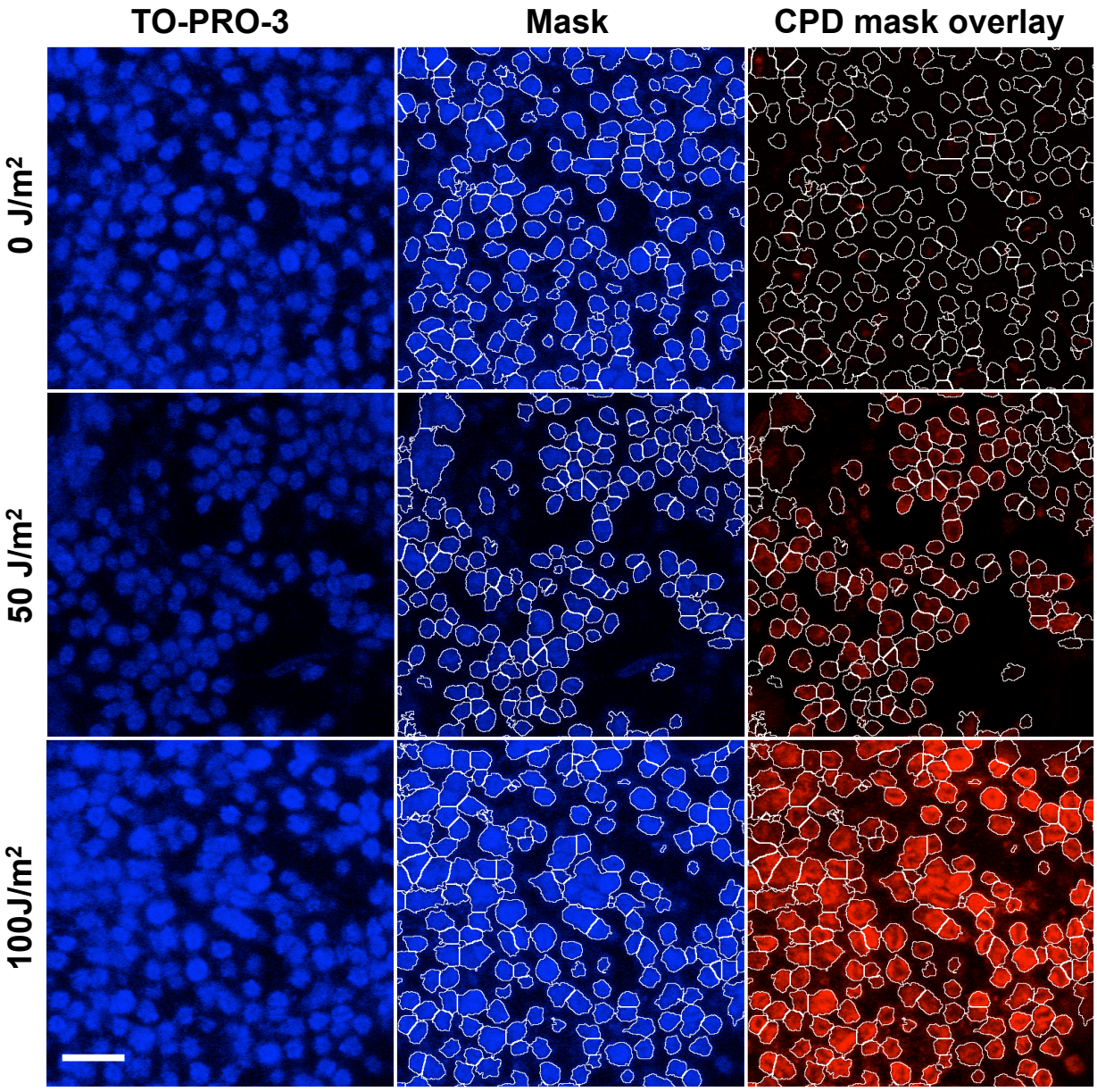

CPD staining was performed as follows: epidermal sheets were permeabilized in PBS containing 0.5% Triton-X100 for 30 min on ice, denatured by a 22 min exposure to 0.4M NaOH in 70% ethanol followed by extensive washing in PBS/ 0.5% Triton-X100. Sheets were then blocked in PBS/0.5% Triton X-100 containing 2% BSA and 1% goat serum, stained with anti-thymine dimer antibody (2 μg/ml, clone H3, Abcam) followed by Alexa-568-goat anti-mouse IgG (Life Technologies) and nuclear staining with To-Pro3 (33 nM, Life Technologies).

For analysis of CPD fluorescence intensity, z-stacked images of 10 fields/ sheet (2 sheets/mouse) were collected in a set pattern with 2mm intervals.

Sample images show masking for the identification and quantification of CPD (red) fluorescence intensity specifically within keratinocyte nuclei. ImageJ software (NIH) was used to create a mask based on TO-PRO3 (blue) nuclear staining, which was then overlaid on the CPD channel to selectively measure fluorescence intensity within nuclei. Scale bar, 20μm

Supplementary Figure S2. Active mutant KC proliferation within p53 islands.

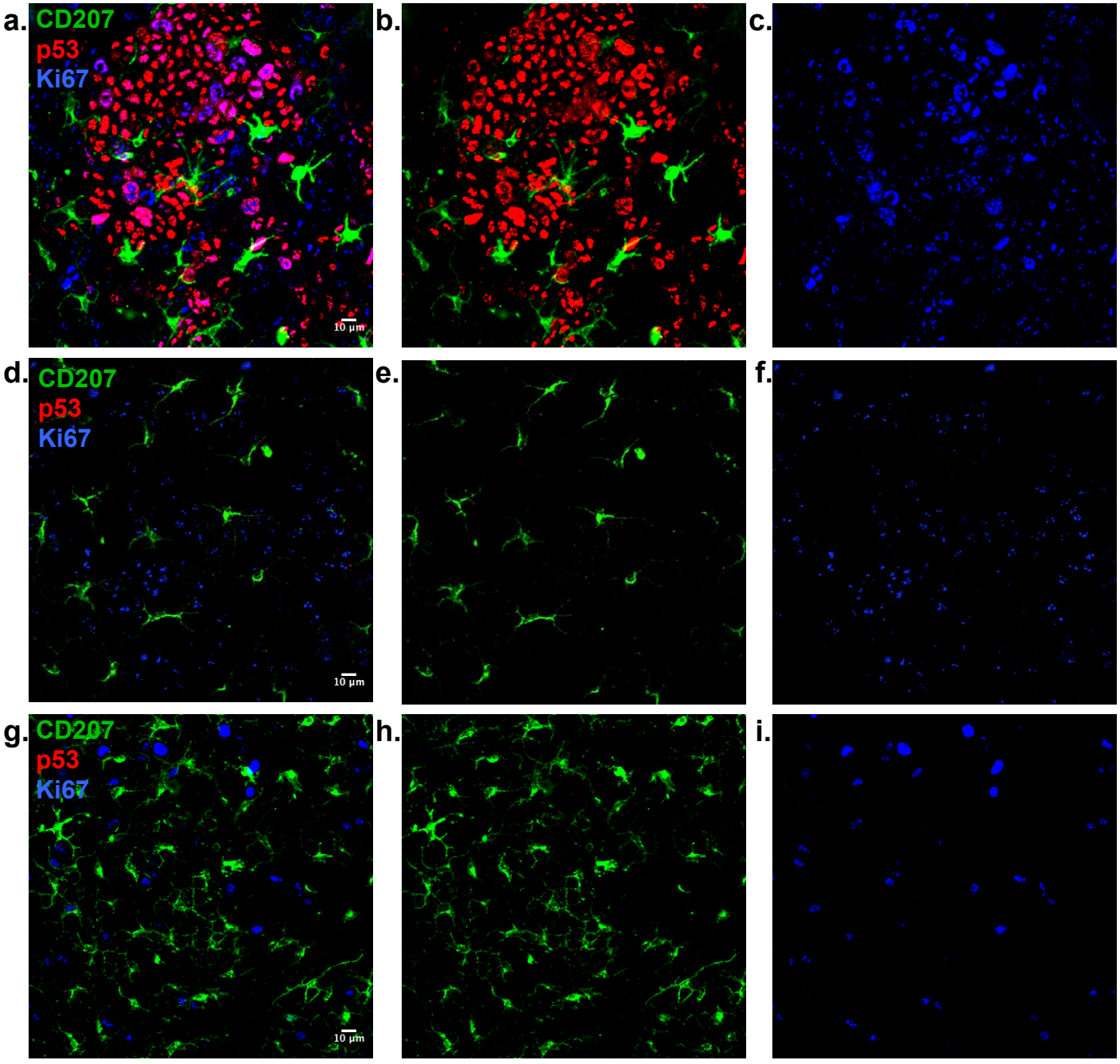

Epidermal sheets prepared from chronic UVB exposed (9 wks, 400 J/m2 3x/wk, panels a - f) or unexposed (panels g - i) FVB.NLC were stained with antibodies to CD207 (green), p53 (red) and Ki-67 (blue). Within each row, the left-most panel is an overlay of all three stains, the center panel overlays CD207 and p53 only, and the right-most panel displays only the Ki-67 channel.

The top row (a – c) is a representative p53 island containing numerous Ki-67+ p53+ proliferating mutant keratinocytes. The center row (d – f) is an area of UVB-exposed skin without a p53 island. The bottom row (g – i) shows baseline proliferation, as well as lack of p53 staining in untreated skin. In all cases, proliferating LC were rarely seen.

Supplementary Figure S3. Identification and measurement of p53 islands and LC.

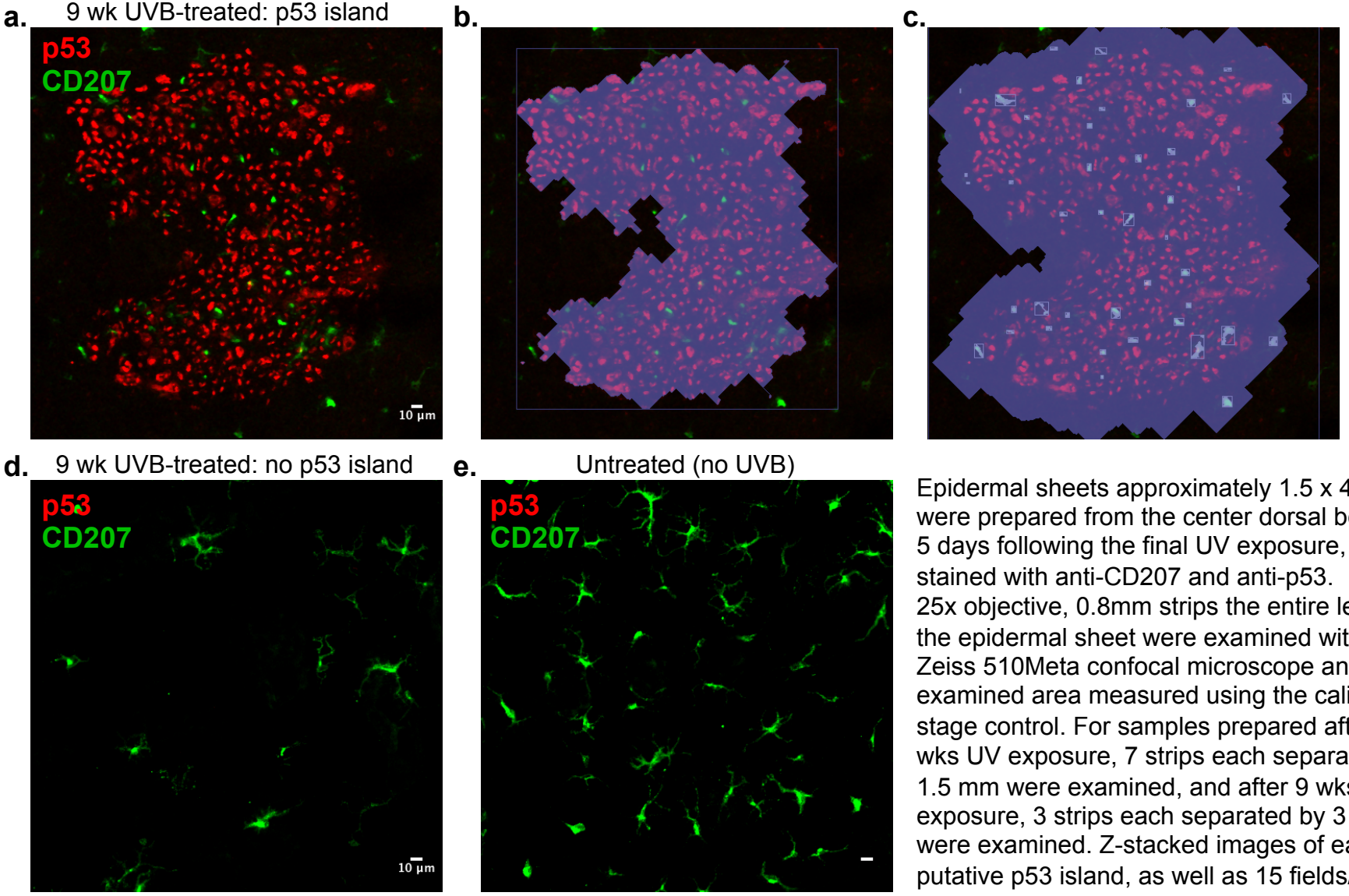

Epidermal sheets approximately 1.5 x 4 cm were prepared from the center dorsal bodywall 5 days following the final UV exposure, and stained with anti-CD207 and anti-p53. Using a 25x objective, 0.8mm strips the entire length of the epidermal sheet were examined with a Zeiss 510Meta confocal microscope and the examined area measured using the calibrated stage control. For samples prepared after 5 wks UV exposure, 7 strips each separated by 1.5 mm were examined, and after 9 wks UV exposure, 3 strips each separated by 3 mm were examined. Z-stacked images of each putative p53 island, as well as 15 fields/ mouse (evenly distributed among the strips examined) where no p53 staining was observed were analyzed using Volocity 6.2 software (Perkin Elmer). A combination of fluorescence intensity and proximity of p53+ nuclei was used to to identify and measure each island (**a, b**). The island perimeter was then expanded by 30 μm (**c**) and CD207+ LC within the expanded perimeter ("island associated") vs those in fields with no p53 staining (**d**) were then identified and quantitated. (**e**) Control, untreated epidermis lacks p53 staining; scale bar = 10 μm.

Supplementary Figure S4. Increased p53 island density and area in the presence of LC in both hairless (hr/hr) and hair-bearing (FVB) mice.

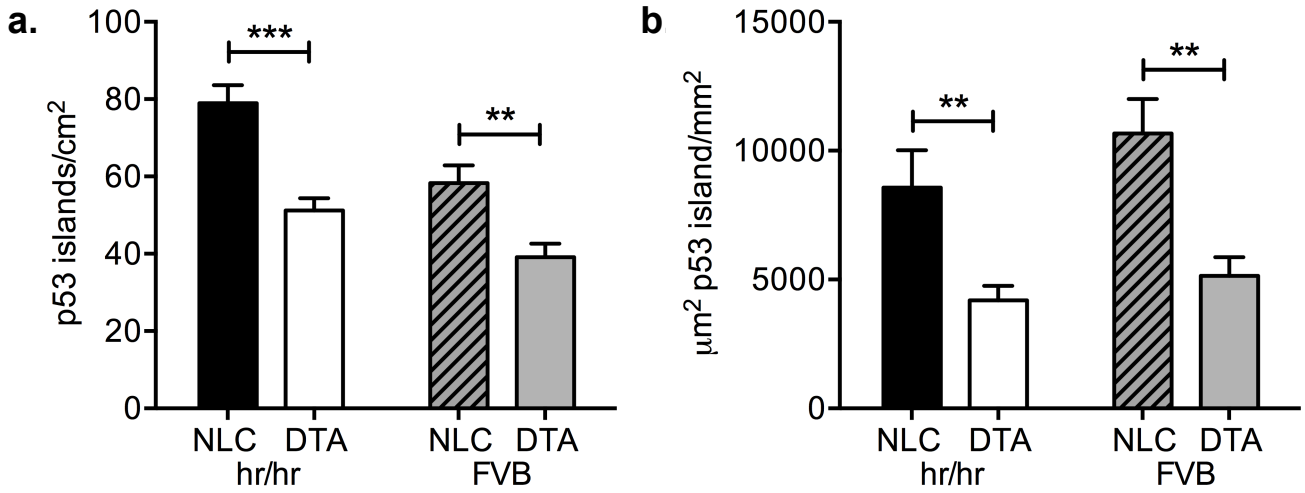

Mutant keratinocyte p53 island density **(a)** and area **(b)** were quantified as described in Supplementary Figure S3 in epidermal sheets prepared following 9 wks chronic UVB exposure (400 J/m^2, 3x/wk). The presence of LC is associated with increased p53 island density and area in both hairless (hr/hr, data from Figure 3 reproduced here) and hair-bearing (FVB) mice. ***P<0.001, **P<0.01.

Supplementary Figure S5. Increased expression of CD207 and MHCII in LC under chronic UVB exposure.

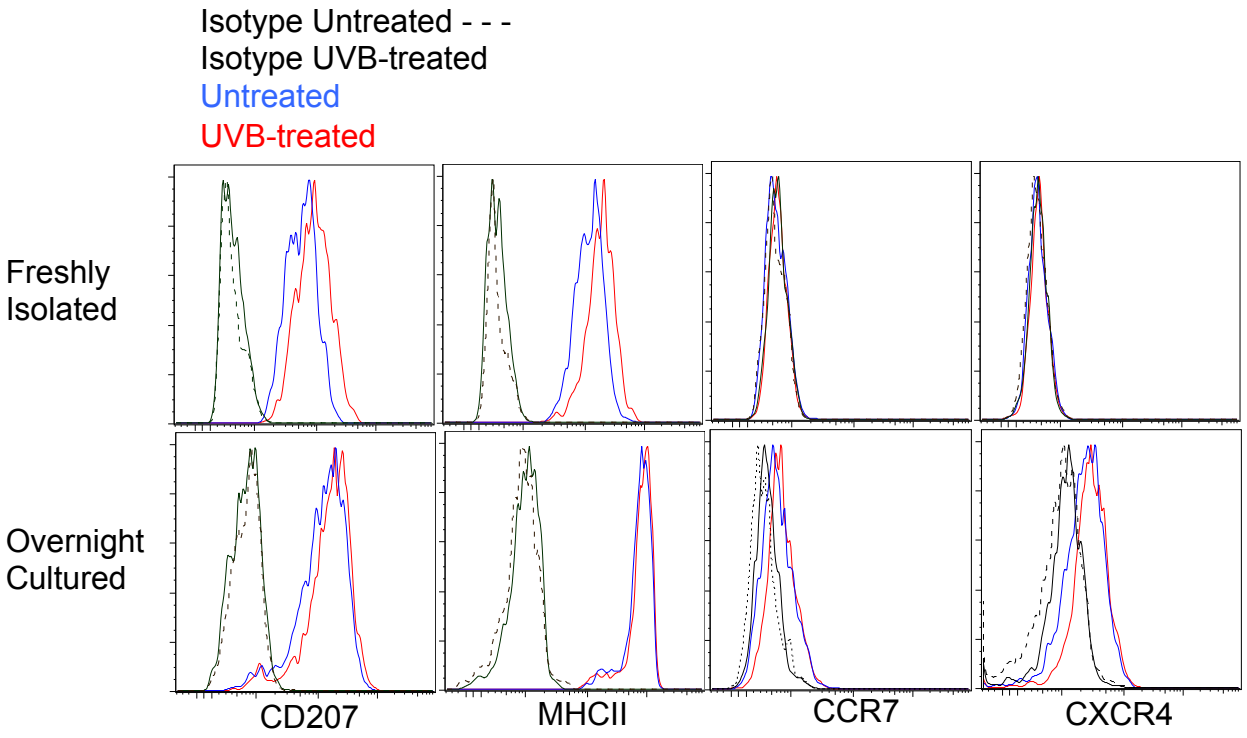

Langerhans cells prepared from individual untreated (blue) vs chronic UVB treated (red) LC-intact (NLC) mice were examined for expression of CD207, MHCII, CCR7 and CXCR4 by flow cytometry, either freshly isolated (top row) or following overnight culture in CRPMI (bottom row). Histograms are gated on CD45+CD207+ epidermal cells and are representative of n=3 mice/group. Freshly isolated LC from chronically UVB treated mice show upregulation of CD207 and MHCII: Mean CD207 ΔMFI untreated = 64.4 ± 2.4, UVB treated = 106.6 ± 2.6, $p = 0.0001$; Mean MHCII ΔMFI untreated = 137.8 ± 3.4, UVB treated = 209.5 ± 2.0, $p < 0.0001$.

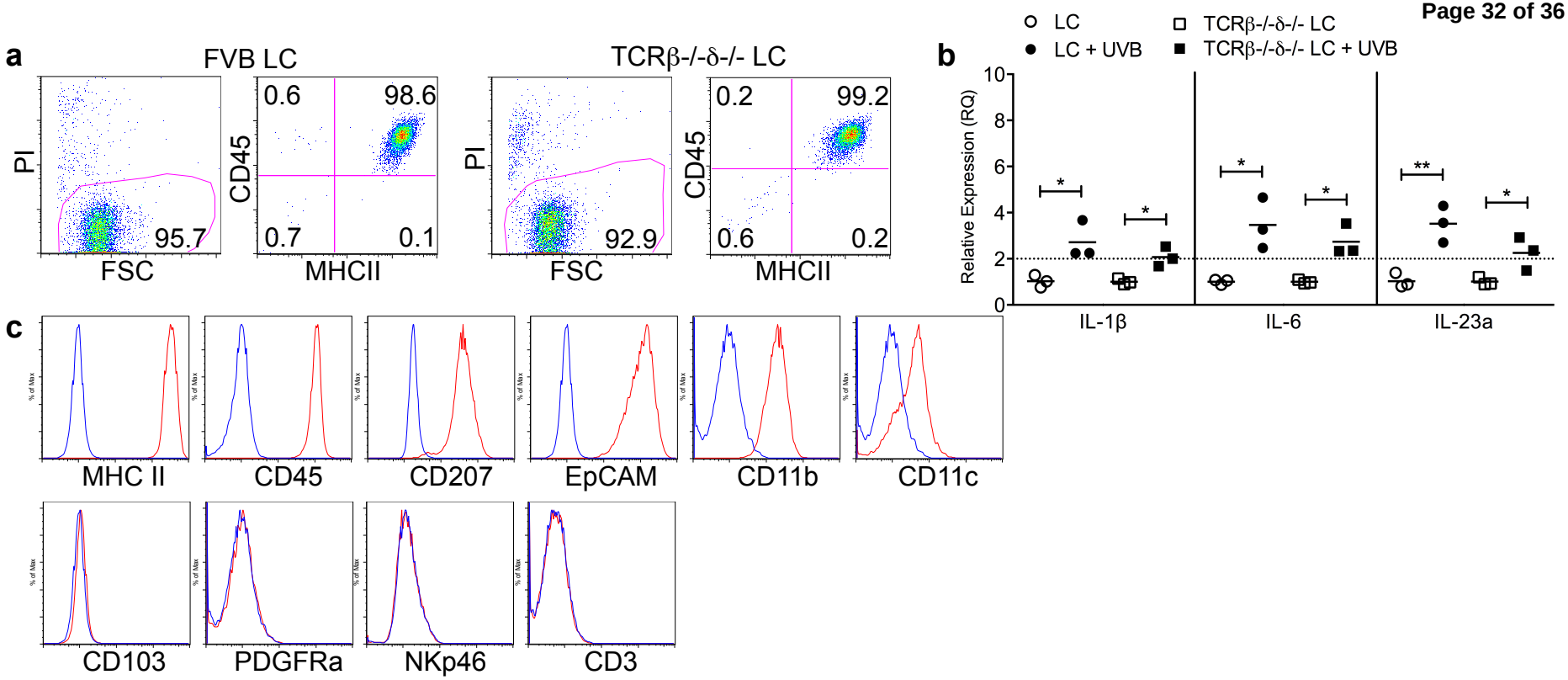

Supplementary Figure S6. (a) Purity of LC isolated from T cell intact (FVB LC) and T cell deficient (TCRβ-/-δ-/- LC) mice as described below. **(b)** Purified LC were cultured for 3 days in CRPMI + 0.5 ng/ml GM-CSF, then left untreated or exposed to 100 J/m^2 UVB and harvested 24hr later. Gene expression relative to untreated LC is shown; each symbol represents one biologic replicate; * P<0.05, **P<0.01. **(c)** Flow cytometric analysis of purified cells from (a) confirms epidermal LC phenotype.

LC preparation and purification. Ear skin from untreated FVB.NLC and TCRβ-/-δ-/-.NLC was incubated in 0.3% trypsin for 1-1.5 hr at 37°C, then whole epidermal sheets lifted away from the dermis and floated basal side down on CRPMI (Modi *et al.*, 2012), containing 0.5 ng/ml GM-CSF (PeproTech, Rocky Hill, NJ). Epidermal sheets were cultured for 4 days at 37°C, then emigrating cells harvested and centrifuged over Lympholyte M (Cedarlane, Burlington, NC). Langerhans cells were then purified using MHCII-magnetic beads (Miltenyi Biotec, San Diego, CA) according to manufacturer's instructions.

Flow cytometry. After blocking FcR (CD16/32) cells were stained with the following antibodies: FITC- or PE-MHC II (M5/114.15.2), PE- or APC-CD45 (30-F11), APC-CD11b (M1/70), APC-CD11c (N418) , APC-CD103 (2E7), APC-CD3 (145-2C11), APC-PDGFRa (APA5) all from eBioscience, or FITC-NKp46 (29A1.4; BD Biosciences), FITC-EpCAM (G8.8; Biolegend), Alexa-488-CD207 (929F3.01; Imgenex). In all cases, isotype-matched control antibodies were used as controls and propidium iodide (PI) included for live cell gating. Data were collected using FACSCalibur (Becton Dickinson) and analyzed with FlowJo (TreeStar, Ashland, OR).

Supplementary Figure S7. Epidermal and dermal dendritic cells in untreated and chronic UVB treated skin.

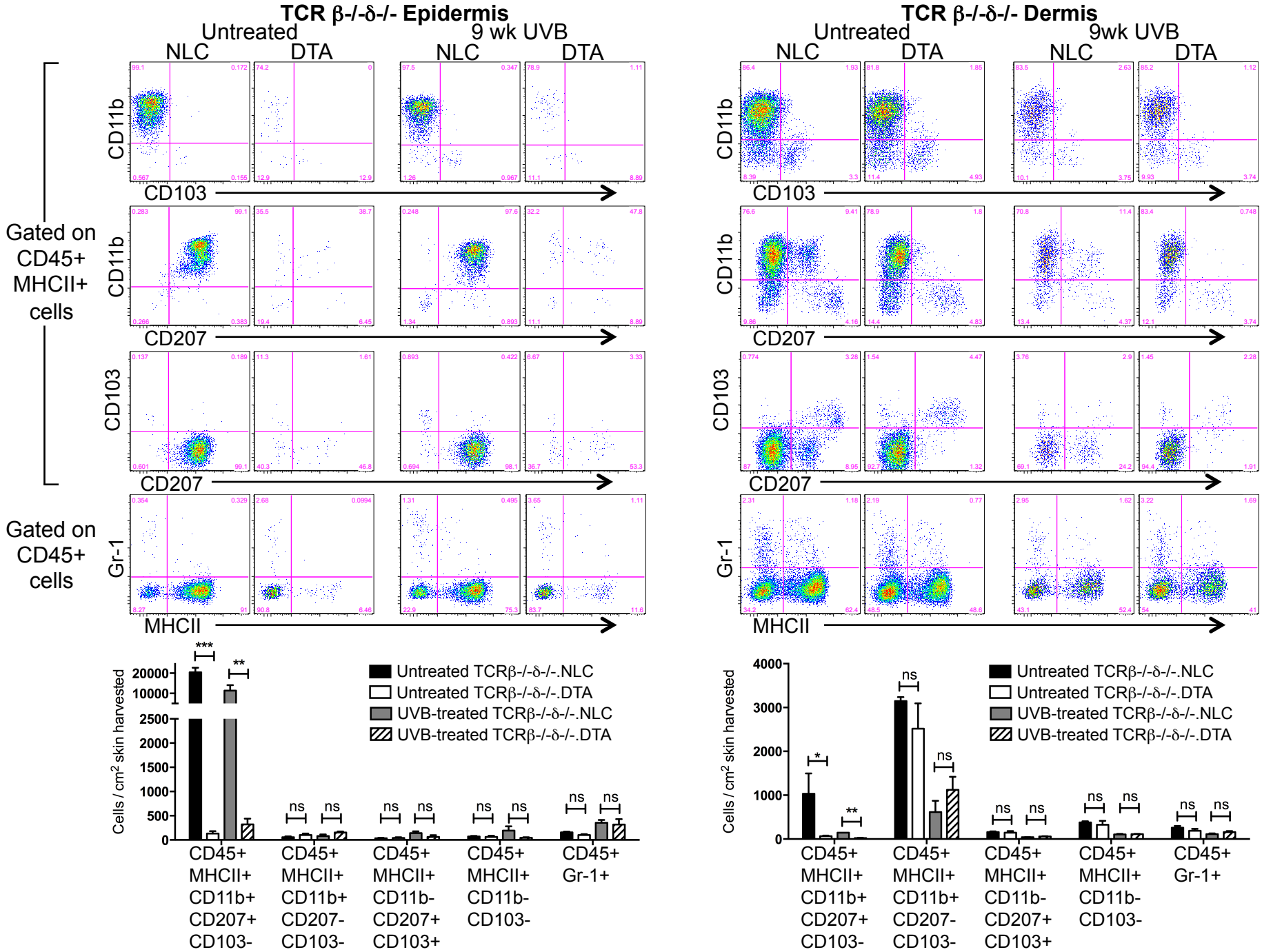

Supplementary Figure S7. Epidermal and dermal dendritic cells in untreated and chronic UVB treated skin.

Epidermal and dermal cell suspensions were prepared from individual untreated and chronic UVB treated (9 wks, 400 J/m^2, 3x/wk) TCRβ-/-δ-/-.NLC and TCRβ-/-δ-/-.DTA mice. Freshly isolated cells were blocked with anti-FcR and stained with the following antibodies: Brilliant Violet 421-CD45 (30-F11, Biolegend), Alexa488-CD207 (929F3.01, Dendritics), PE-MHCII (M5/114.15.2, eBioscience), APC-CD11b (M1/70, eBioscience), PE-Cy7-CD103 (2E7, Biolegend) or isotype matched controls, along with the viability dye EMA. Flow cytometric data were collected on Stratedigm S1000EX and analyzed with FlowJo. CD207, CD11b and CD103 dot plots (top three rows) are gated on viable, single, CD45+ MHCII+ cells and these stains used to define major dendritic cell populations in epidermis and dermis: LC: CD45+ MHCII+ CD11b+ CD207+ CD103-; CD11b dermal DC: CD45+ MHCII+ CD11b+ CD207- CD103-; CD103 dermal DC: CD45+ MHCII+ CD11b- CD207+ CD103+; other DC: CD45+ MHCII+ CD11b- CD103-. Additional samples were also stained with APC-Gr-1 (RB6-8C5, eBioscience) to identify infiltrating monocytes or neutrophils (bottom row dot plots, gated on viable, single CD45+ cells). Absolute cell numbers (shown in bar graphs) were calculated by multiplying the percent marker positive by the previous gates (i.e. CD45+MHCII+, single and viable) by viable cell yield (trypan-blue excluding cells) and dividing this by the measured area of skin harvested. Plots are representative individuals of n=3 mice/group. *** $P \leq 0.001$, ** $P \leq 0.01$, * $P \leq 0.05$ by Student's t-test.

Supplementary Figure S8. Epidermal ILC Phenotype

Gated on CD45+ MHCII- TCRβ-/-δ-/- epidermal cells

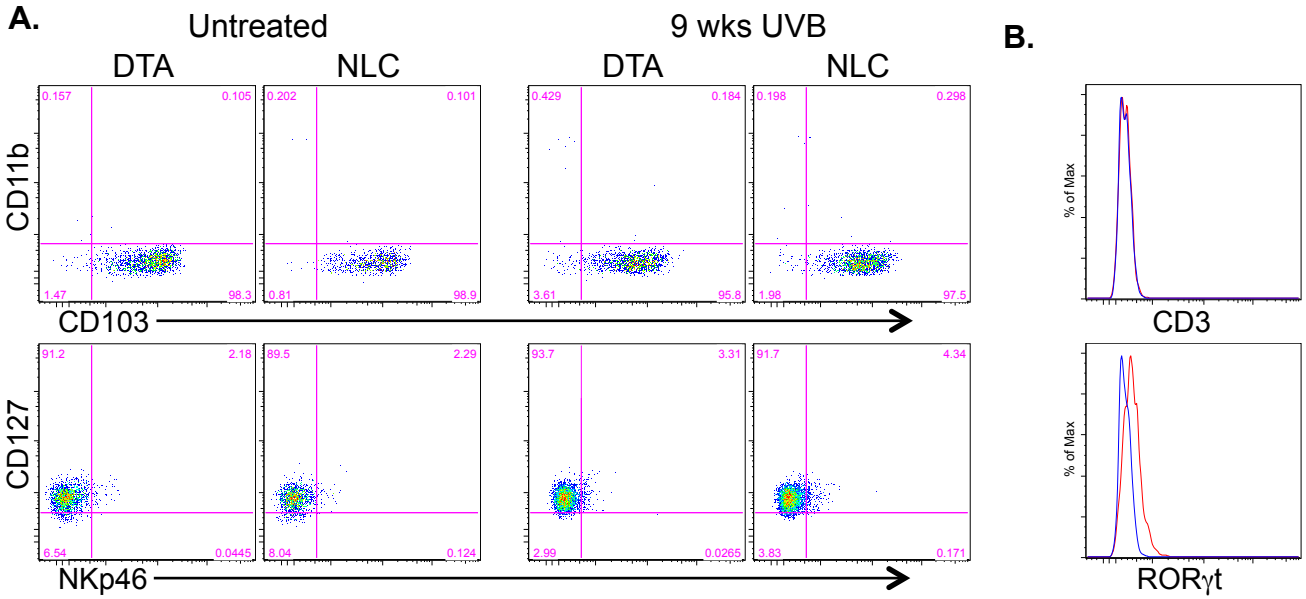

A. Epidermal cell suspensions were prepared from individual untreated and chronic UVB treated (9 wks, 400 J/m^2, 3x/wk) TCRβ-/-δ-/-.NLC and TCRβ-/-δ-/-.DTA mice. After blocking FcR, cells were stained with the following antibodies: Brilliant Violet 421-CD45 (30-F11, Biolegend), FITC-NKp46 (29A1.4, BD Biosciences), PE-MHCII (M5/114.15.2, eBioscience), APC-CD11b (M1/70, eBioscience), PE-Cy7-CD103 (2E7, Biolegend) or PE-Cy7-CD127 (IL7Ra, A7R34, Biolegend) or isotype matched controls, along with the viability dye EMA. Spleen cells were stained as a positive control for NKp46 (not shown). Flow cytometric data were collected on Stratedigm S1000EX and analyzed with FlowJo. Plots are representative individuals of n=3 mice/group.

B. Epidermal cell suspensions prepared from untreated TCRβ-/-δ-/-.NLC mice. After blocking FcR, cells were stained with the viability dye EMA, Brilliant Violet 421-CD45 (30-F11, Biolegend), PE-MHCII (M5/114.15.2, eBioscience) and PE-Cy7-CD3 (145-2C11, Biolegend), fixed and permeabilized using Cytofix/Cytoperm (BD), then stained with APC-RORγt (B2D, eBioscience) or isotype matched controls. CD45+ MHCII- epidermal cells from TCRβ-/-δ-/- mice lack CD3, and express the ILC3-associated transcription factor RORγt.

Supplementary Figure S9. Langerhans cells facilitate abrasion-induced IL-22 gene expression.

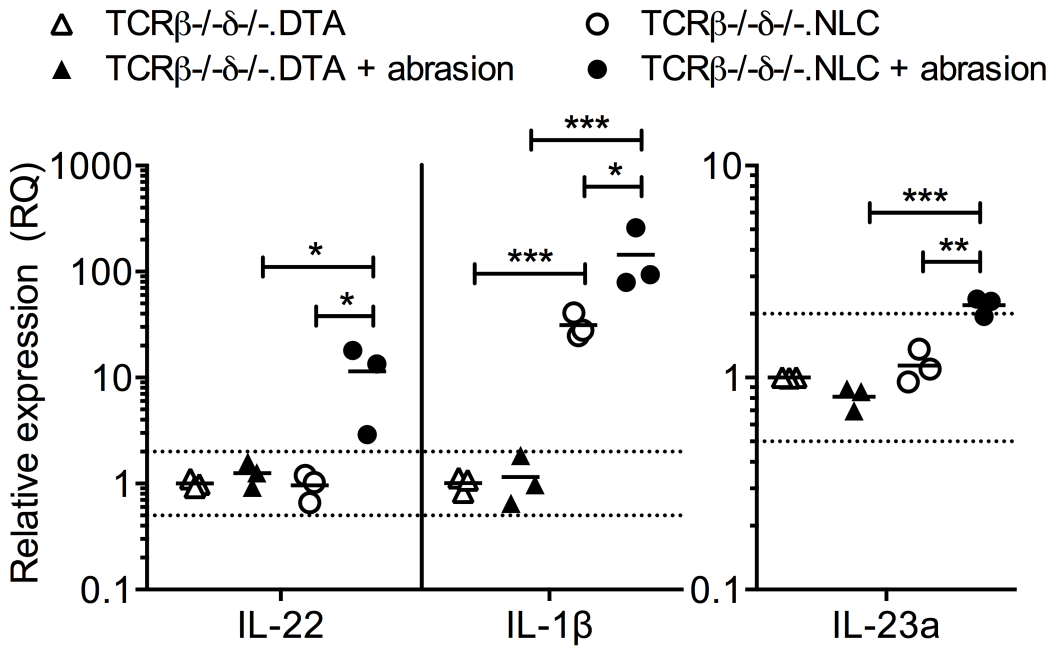

Epidermal cell suspensions prepared from untreated or razor abrasion-treated (48 hr) TCRβ-/-δ-/-.NLC and TCRβ-/-δ-/-.DTA mice were examined for changes in gene expression by quantitative real-time PCR. Gene expression relative to untreated TCRβ-/-δ-/-.DTA epidermal cells is shown; each symbol represents one mouse. Statistical significance was determined using Holm-Sidak correction for multiple comparisons, *P<0.05, **P<0.01, ***P<0.001.